



ELSEVIER

Journal of Molecular Catalysis A: Chemical 162 (2000) 135–145



www.elsevier.com/locate/molcata

Dinitrogen as probe molecule of alkali-exchanged zeolites A density functional study

Georgi N. Vayssilov^{*}, Anguang Hu, Uwe Birkenheuer, Notker Rösch¹*Institut für Physikalische und Theoretische Chemie, Technische Universität München, 85747 Garching, Germany*

Dedicated to Professor Helmut Knözinger on the occasion of his 65th birthday.

Abstract

The binding energies and adsorption induced vibrational frequency shifts of N_2 molecules adsorbed on alkali-exchanged zeolites were calculated using a density functional method. Both on bare cations and at model zeolite clusters, linear adsorption of probe molecules at the extra-framework metal cations was found to be the most stable configuration. Depending on the alkali cation, adsorption is accompanied by a blue-shift of $10\text{--}25\text{ cm}^{-1}$ of the N–N stretching mode. The calculations support the experimental observation of simultaneous adsorption of two N_2 molecules on one alkali cation. The calculated frequency shifts of the N–N mode of the bis-dinitrogen complex on a Na-exchanged zeolite is by 4 cm^{-1} lower than for the corresponding monomolecular adsorption model while the position of the band is almost unchanged for the K-exchanged model. For different alkali cations, the frequency shift was found to be proportional to the intensity of the N–N stretching mode. Using calculated frequency shifts and experimental values for N_2 adsorbed on a series of alkali-exchanged zeolites, a reference value for the IR vibrational frequency of a non-interacting N_2 molecule in zeolite cages was derived. This suggests that a more precise determination of the reference frequency will be feasible once a consistent set of experimental data for both isotope molecules $^{14}N_2$ and $^{15}N_2$ adsorbed on the same series of alkali-exchanged zeolites, with intensity values measured by a uniform method, is available. © 2000 Published by Elsevier Science B.V.

Keywords: Alkali cation exchanged zeolites; Nitrogen adsorption; OF study; Bis-dinitrogen complex; Vibrational frequencies; IR intensities

1. Introduction

The accurate characterization of metal cations in alkali-exchanged zeolites is essential for understanding and predicting specific properties of these materials as catalysts and sorbents [1]. Alkali cations in zeolite cavities act as Lewis acid centers and interact with basic groups of adsorbed molecules [2,3]. We

recently demonstrated the importance of this type of interaction for the example of methanol adsorbed on sodium exchanged zeolites [4]; about 80% of the calculated binding energy of the guest molecule to an active site derives from the co-ordination of the methanol oxygen center to the alkali cation, while only 20% is due to a hydrogen bond with an oxygen center of the zeolite framework. Therefore, it is important to establish the acidity strength of cationic active sites.

A well established technique for elucidating the location and properties of metal cations in oxides and zeolites is IR spectroscopy of weakly interacting

^{*} Corresponding author. Present address: Faculty of Chemistry, University of Sofia, BG-1126 Sofia, Bulgaria.

E-mail address: gnv@chem.uni-sofia.bg (G.N. Vayssilov).

¹ Co-corresponding author.

adsorbed probe molecules [5–9] — carbon monoxide, molecular nitrogen or hydrogen. The vibrational frequency shift of these adsorbed molecules is essentially due to their polarization in the field of the metal cation and the stretching frequency peak position provides information on the location and acidity of the cation. In addition, these small diatomic molecules are not influenced by interaction with basic oxygen centers that exist in alkali zeolites [10]. In a previous theoretical paper [11], we investigated the peculiarities of carbon monoxide as probe molecule for cations in sodium-exchanged zeolites. Here, we extend this investigation with modeling the adsorption of N_2 on cationic centers in zeolites as an alternative IR probe molecule. Since N_2 does not have a genuine dipole moment, its stretching vibration is IR active only upon interaction with a polarizing system. When employed for the characterization of alkali cations, not only the frequency but also the intensity of the corresponding IR band depends on the electric field generated by the cation [12]. Exploiting this peculiarity, dinitrogen adsorption has successfully been used for identifying small amounts of lighter alkali cations (such as Na^+) in the presence of heavier ones (e.g. Rb^+) [13]. Despite of the weak adsorption of N_2 molecules at alkali cations in zeolites, bis-dinitrogen complexes recently have been observed on the alkali forms of zeolites Y [14,15], EMT [16], and ETS [17]. In these cases, calculations are helpful to estimate the adsorption energy of dinitrogen at the metal cations and to check the correspondence of the frequency shifts in mono- and bis-dinitrogen complexes to the experimental values. Similar model calculations successfully reproduced the vibrational frequency shift of N_2 molecules interacting with OH groups of the acidic forms of zeolites [18,19].

In the present work, we investigate computationally the interaction of one or two N_2 probe molecules with bare alkali cations and with Na^+ or K^+ cations coordinated to a zeolite model ring. In these model calculations, we use a six-ring containing two aluminum atoms, which are typical for Y zeolites [20,21]. Moreover, we found that the adsorption of CO on a sodium cation located at this type of ring [11] produces the most intense peak in the experimental IR spectra [22]. We also calculate the harmonic vibrational frequencies and band intensities

and we compare them with the experimental spectra for both nitrogen isotopes ^{14}N and ^{15}N .

2. Method

The zeolite fragment is modeled as a six-ring of a faujasite structure which contains two aluminum centers in *para* position (cf. Fig. 1). This cluster, designated as Al-2p [11], has already been used in our study of CO adsorption. Free valences of the silicon and aluminum atoms in the ring are saturated by hydrogen atoms. The initial positions of the T-atoms and the oxygen centers in the six-ring were taken from average crystallographic values [23]. The excess negative charge of the clusters due to the presence two Al atoms and only one mono-valent alkali cation was compensated by a proton connected to an oxygen center of a Al–O–Si bridge which is directed outward from the ring in order to minimize the direct effect of the compensating cation on the central alkali ion. In both cation containing model clusters, Na–Al-2p and K–Al-2p, the positions of the oxygen centers of the ring, the alkali cation, and the charge-compensating proton were optimized, keeping the positions of the T-atoms fixed. Details of the charge compensation procedure have been discussed elsewhere [11].

The positions of the alkali and framework oxygen centers were re-optimized after adsorption of one or two probe N_2 molecules at the cationic site of the cluster model. No symmetry constraint was applied for adsorption at cluster models and linear adsorption at bare cations, while the structures for ‘side-on’ adsorption of N_2 at bare cations with two equal M–N distances were optimized in C_{2v} symmetry.

The calculations were carried out with the new density functional (DF) program PARAGAUSS [24] using the gradient corrected exchange–correlation functional suggested by Becke (exchange) [25] and Perdew (correlation) [26]. Gaussian-type basis sets, contracted in generalized form, were employed to describe the Kohn–Sham orbitals: (6s1p) → [3s1p] for H, (9s5p1d) → [5s4p1d] for O and N, (12s9p1d) → [6s4p1d] for Al and Si, (12s8p1d) → [6s5p1d] for Na, and (15s11p1d) → [6s5p1d] for K [27,28]. Relativistic effective core potentials (ECP) were adopted for Rb and Cs [29,30].

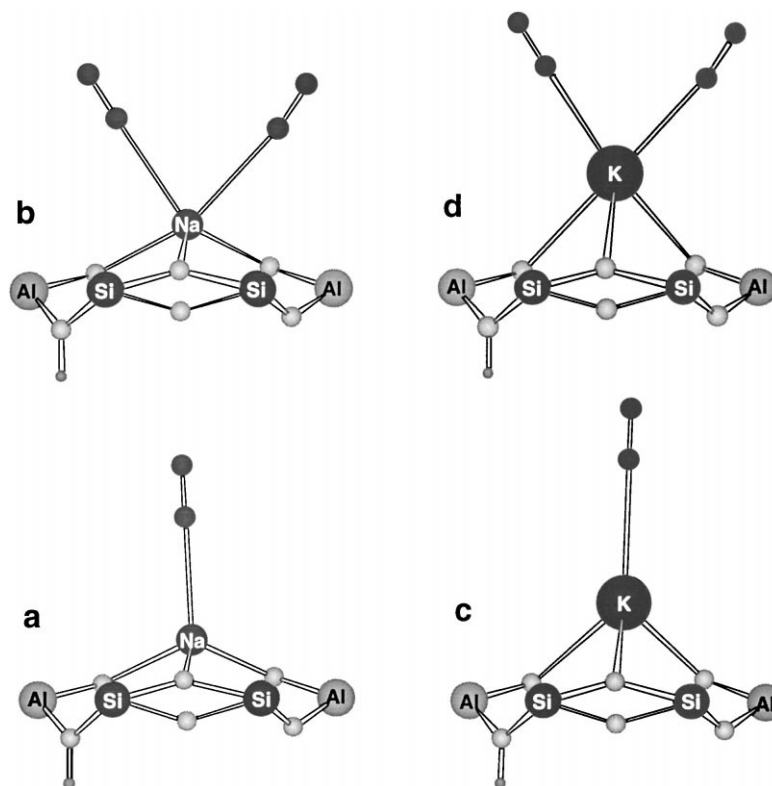


Fig. 1. Optimized structures for mono- and bi-molecular adsorption of N_2 at the model clusters Na–Al-2p and K–Al-2p. The plane of the T-atoms in the six-ring is perpendicular to the plane of the drawing, i.e. the other two Si centers are exactly behind the two Si centers shown in the front.

The structures of the clusters described above were optimized automatically using analytical energy gradients [30,31]. After optimization of a cluster model, a constrained frequency analysis was carried out where the vibrational modes related to the adsorbed probe molecules and the alkali cation were taken into account. Normal harmonic vibrational frequencies were calculated by diagonalizing the mass weighted force constant matrix in internal coordinates. The force constants were obtained numerically by finite differences of analytical energy gradients.

3. Results and discussion

3.1. N_2 adsorption at bare alkali cations

The calculated binding energies (BE) and structural parameters for a nitrogen molecule coordinated

to bare alkali cations are shown in Table 1. The calculated BE values indicate that for all alkali cations linear adsorption of dinitrogen is preferred over side-on structures. The ratio between BE(linear) and BE(side-on) is lowest for Na^+ and K^+ , about 3; for larger cations the BE for side-on adsorption is negligible (Table 1). One should keep in mind that common exchange–correlation functionals are not accurate enough [32,33] for describing weak interactions with binding energies of 20 kJ/mol or less. The calculated BE values should represent lower bounds since attractive contributions of dispersion interactions (albeit small in the present case) are not reproduced by the common approximate exchange–correlation functionals. In any case, the trends derived from the values of Table 1 are expected to remain correct even after dispersion interaction is taken into account.

Table 1
Calculated characteristics^a of N₂ molecules adsorbed at bare alkali cations

Cation	BE	1/s ^b	R(M–N)	ΔR(N–N) ^c	Δν(¹⁴ N ₂) ^c	I(¹⁴ N ₂)	ν(M– ¹⁴ N)	k(M–N)	Δν(¹⁵ N ₂) ^c
Linear									
Li ⁺	58	3.9	213.1	–0.2	24.4	55	336.2	29.4	23.6
Na ⁺	40	3.1	247.6	–0.2	18.9	41	176.0	15.1	18.3
K ⁺	26	2.9	298.5	–0.2	13.3	30	101.4	5.9	12.9
Rb ⁺	19	4.9	322.2	–0.1	11.5	25	89.2	5.4	11.1
Cs ⁺	15	5.0	351.7	–0.1	9.5	22	60.6	2.6	9.2
2N ₂ –Na ⁺	78		249.1	–0.2	9.4, 14.0	0, 29	119, 216		9.4, 13.8
Side-on									
Li ⁺	15	263.2	0.2	–15.2					
Na ⁺	13	289.5	0.1	–9.7					
K ⁺	9	345.0	0.0	–4.0					
Rb ⁺	4	405.4	0.0						
Cs ⁺	3	428.8	0.0						

^a Dinitrogen binding energies (BE) to alkali cations in kJ/mol, metal-nitrogen distances *R*(M–N) and changes Δ*R*(N–N) of the N–N distance with respect to free N₂ in pm, harmonic vibrational frequency shifts Δν(N–N) with respect to free N₂ and harmonic vibrational frequency ν(M–N) in cm^{–1}, intensity *I* of the N–N band in km/mol, force constant *k*(M–N) in N/m.

^b Ratio between the binding energies of linear and side-on adsorption complexes of dinitrogen.

^c Calculated parameters for free N₂: *R*(N–N) = 111.1 pm, ν(¹⁴N–¹⁴N) = 2320.7 cm^{–1}, ν(¹⁵N–¹⁵N) = 2242.0 cm^{–1}.

The BE calculated for the linear complex N₂–Na⁺, 40 kJ/mol, is higher than the value calculated for adsorption of carbon monoxide at Na⁺, 31 kJ/mol [11]. The strength of the interaction of a N₂ molecule with different alkali cations decreases with increasing atomic number as can be seen from the variation of the BE for linear adsorption: from Li⁺ to Cs⁺, the BE is reduced from 58 to 15 kJ/mol (Table 1). The interaction of a CO molecule with the cation leads to a shortening of the C–O bond by about 1 pm [11], while the N–N bond of a N₂ molecule coordinated to Na⁺ cation is only 0.2 pm shorter than that of free N₂. Thus, the N–N bond in the coordinated molecule is only slightly stronger, compared to the free molecule. Tiny changes of the N–N bond length in this series of alkali cations, by 0.1 pm, indicate a weakening of the N–N bond when going from Li⁺ to Cs⁺.

Similar to CO adsorption, the intramolecular vibrational frequency for N₂ molecule coordinated to alkali cations increases with respect to free molecule (Table 1). In addition to the weak stabilization of the N–N bond in the adsorption complex, the blue shift of the band is likely due to the so-called ‘wall’ effect [34,35] caused by Pauli repulsion of the closed electronic shells of the probe molecule and the cation. In fact, a vibrational red-shift and an elongated N–N

bond is found for the less stable side-on coordination of N₂ molecule to a sodium cation. In the series of alkali cations, the calculated blue-shift with respect to the calculated frequency of the free N₂ molecule decreases from 24.4 cm^{–1} for ¹⁴N₂–Li⁺ to 9.5 cm^{–1} for ¹⁴N₂–Cs⁺. This order agrees with the expected influence of the dimensions of the alkali cation on the Pauli repulsion: small, hard cations exhibit a larger blue-shift than larger, softer cations.

The calculations also reveal a linear correlation between the N–N band intensity *I*(N–N) and the frequency shift Δν(N–N) (Fig. 2a). Both parameters depend on the square of the field strength of the cation as estimated by the reciprocal value of the square of the M–N distance, according to Coulomb’s law (Fig. 2b). Such a quadratic dependence of the vibrational frequency ν(N–N) on the M–N distance, as estimated by the ionic radii of the cations and the radius of the probe molecule, has previously been discussed for experimental values [36].

A linear structure of the adsorption moieties N₂–Na⁺ (symmetry D_{∞h}) is also found to be the most stable one when two N₂ molecules are coordinated simultaneously to one Na⁺ center. The BE per each molecule, 39 kJ/mol (Table 1), is essentially the same as in monomolecular adsorption, 40 kJ/mol. In the bis-dinitrogen complex, the N–N stretching mo-

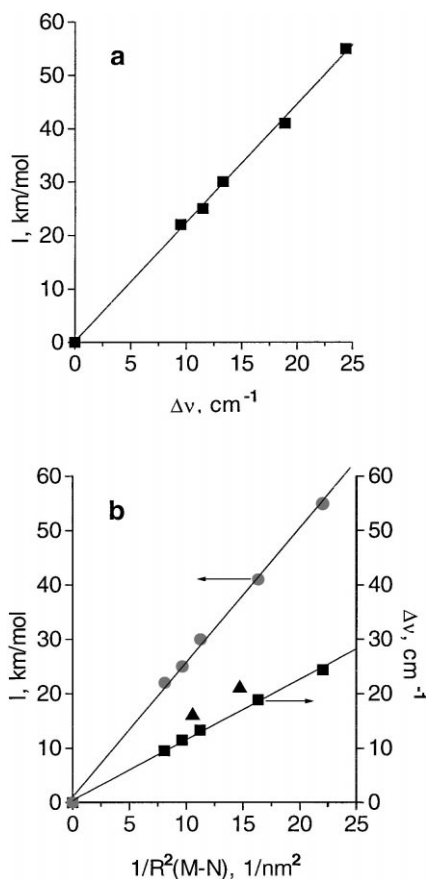


Fig. 2. (a) Linear correlation between the calculated values of the intensity I and the frequency shift $\Delta\nu$ of the N–N stretching mode of a dinitrogen molecule coordinated to alkali cations. (b) Dependence of the frequency shift $\Delta\nu$ (squares, left-hand axis) and the intensity I (circles, right-hand axis) on the electric field strength of the cation as estimated by the reciprocal value of the square of the distance $R(M-N)$. The frequency shifts $\Delta\nu$ of N_2 on the cluster models Na–Al-2p and K–Al-2p are marked by triangles. The correlation coefficients of all straight lines are 0.99.

tions form symmetric and antisymmetric modes with blue-shifts of 9.4 and 14.0 cm^{-1} , respectively; both frequencies are lower than the shift of the monomolecular adsorption complex.

The frequency of the $\nu(\text{N}-\text{M})$ mode decreases with the size of the cation, from 336 cm^{-1} for Li^+ to 61 cm^{-1} for Cs^+ (Table 1). The corresponding force constants also decrease in this order (Table 1). The N–Na band for monomolecular adsorption of N_2 is calculated at 176 cm^{-1} . When two nitrogen molecules are adsorbed, this N–Na band splits into

symmetric and antisymmetric components, at 119 and 216 cm^{-1} (for $^{14}\text{N}_2$). The frequency of the $\nu(\text{N}-\text{M})$ mode depends also on the nitrogen isotope used in the probe molecule. The calculated $\nu(\text{N}-\text{M})$ frequencies for adsorption of a $^{15}\text{N}_2$ molecule are by $2-3\text{ cm}^{-1}$ lower than those for a $^{14}\text{N}_2$ molecule.

3.2. N_2 adsorption at zeolite model clusters

The optimized structures for mono- and bi-molecular adsorption of N_2 at the cluster models Na–Al-2p and K–Al-2p are shown in Fig. 1 and the corresponding distances are reported in Table 2. The BE values for the adsorption of one N_2 molecule on Na–Al-2p and K–Al-2p clusters, 18 and 17 kJ/mol , respectively, are lower than for N_2 coordination at the corresponding bare cations (Table 1), similar to what has been found for CO adsorption on zeolite cluster models [37]. Yamazaki et al. [38] reported 28 and 24 kJ/mol for the heat of adsorption of N_2 on NaZSM-5 and KZSM-5 zeolites, respectively. The difference of $7-10\text{ kJ/mol}$ between the experimental and calculated values is likely caused by shortcomings of the exchange–correlation functional used (see above). The dispersive van der Waals-type interactions of the probe molecule with the zeolite framework [33] which is not accounted for by the isolated cluster model used in our calculations is expected to be negligible because the probe molecules are very small. Thus, they would exhibit little direct contact with the (missing) zeolite framework. Upon adsorption of the probe molecule, the cation moves 10 pm farther from the zeolite ring which leads to enlarged distances between Na^+ and the zeolite oxygen centers.

For the second N_2 molecule, an adsorption energy of 16 kJ/mol is calculated at the cluster models of both cations; this value is close to the BE values of the first probe molecule. In the cluster Na–Al-2p, the cation shifts farther from the zeolite, by 12 pm , likely because of the repulsion between the two adsorbed probe molecules and the zeolite ring. The shift of K^+ upon adsorption at the cluster K–Al-2p is the same for one or two probe molecules, 7 pm . This cation is larger; thus, it is already far from the zeolite ring, at 203 pm in the initial cluster, and it offers more space to additional ligands.

Table 2
Characteristics^a of nitrogen molecules adsorbed at zeolite-embedded alkali cations^b

Cluster	Na zeolite		K zeolite		
	1 N ₂	2 N ₂	1 N ₂	2 N ₂	
BE	18	34	17	33	
$\Delta R(\text{N-N})$	-0.2	-0.2	-0.2	-0.2	
Z ^c	122	134	210	210	
$R(\text{M-N})$	261.2	277.0; 269.9	307.9	311.1; 308.5	
$\alpha(\text{M-N-N})$	179.6	170.2; 178.8	179.4	175.0; 170.4	
$\alpha(\text{N-M-N})$		76.9		81.3	
$I(^{14}\text{N}_2)$	1.9	2.7; 2.2	1.4	2.5; 2.1	
$\Delta\nu(^{14}\text{N}_2)^{\text{d}}$	calc.	20.7	15.3	14.8; 16.1	
	exp. ^e	15.0	13.0	13.0	
$\Delta\nu(^{15}\text{N}_2)^{\text{d}}$	calc.	20.3	14.7	14.3; 15.6	
	exp. ^f	18.5	15.5		
	exp. ^g	18.5	15.0	12.0	11.5
$\nu(^{14}\text{N}-^{15}\text{N})$	calc.	2300.4	2296.8		
$\nu(^{15}\text{N}-^{14}\text{N})$	calc.	2300.1	2296.6		
$\nu(\text{M}-^{14}\text{N}_2)$	calc.	129.4	95; 113	93.6	79.6; 75.1

^a Dinitrogen binding energies (BE) in kJ/mol, distances R in pm, angles α in degrees, harmonic vibrational frequencies ν in cm^{-1} , intensities I in km/mol .

^b Frequencies shifts of relevant experimental bands are also provided.

^c Distance Z of the metal cations to the plane of the T-atoms in pm; the values of the initial clusters are 112 pm for Na-Al-2p and 203 pm for K-Al-2p.

^d Vibrational frequency shifts $\Delta\nu(\text{N-N})$; experimental shifts with respect to the reference values ν_0 for non-interacting N₂ derived in Fig. 3: 2318 cm^{-1} for $^{14}\text{N}_2$ and 2240 cm^{-1} for $^{15}\text{N}_2$; calculated shift with respect to free N₂: 2320.7 cm^{-1} .

^e Experimental data for $^{14}\text{N}_2$ on ETS; from [17].

^f Experimental data for $^{15}\text{N}_2$ on NaY zeolite; from [14].

^g Experimental data for $^{15}\text{N}_2$ on EMT; from [16].

When only one N₂ molecule is adsorbed at the cluster models, it coordinates in linear fashion to the cation (the M-N-N angle is $180 \pm 0.6^\circ$), almost perpendicular to the zeolite ring (Fig. 1a and c). The interatomic distances Na-N and K-N increase by 13 and 9 pm, respectively, compared to adsorption at bare cations, while the N-N bond shortens (relative to the gas phase) by the same amount as on bare cations, 0.2 pm. No stable configuration was found for probe molecules adsorbed in side-on fashion to cations at the zeolite ring models.

The two probe molecules in the bi-molecular adsorption complexes (Fig. 1b and d) are almost equivalent. The angle N-Na-N is slightly more acute, 77° , compared to 81° for the potassium containing cluster, since the sodium cation is closer to the zeolite ring and the repulsion between the zeolite oxygen centers and the probe molecules is stronger.

In Table 2, we report the calculated vibrational frequency shifts for both $^{14}\text{N}_2$ and $^{15}\text{N}_2$ molecules to assist in the comparison with the corresponding experimental data for both isotope molecules [13,14,16,17,36,38]. At variance with CO adsorption, the vibrational frequency shift of a N₂ molecule at cations embedded in zeolite clusters is almost the same as at bare ions, Na⁺ and K⁺. The blue-shift of the N-N stretching band for monomolecular adsorption is about 21 and 15 cm^{-1} for the clusters Na-Al-2p and K-Al-2p, respectively. Since the M-N distance of N₂ adsorbed on Na and K cations of zeolite clusters increases, the Pauli repulsion contribution to the blue-shift of the N-N vibrational band should decrease with respect to the value calculated for coordination on bare cations. However, this effect is compensated by an additional contribution to the N-N blue-shift, the repulsion between the adsorbed

molecule and the zeolite cluster. In the case of bimolecular adsorption, the N–N stretching vibrations of the two adsorbed molecules have slightly different frequencies (by about 1.4 cm^{-1}) at both clusters, Na–Al-2p and K–Al-2p. Due to the weak M–N bonding, this is not a splitting of the band into symmetric and antisymmetric parts but rather originates from tiny differences in the bonding and orientation of the two adsorbed molecules with respect to the zeolite oxygen centers. Since the difference is small, the two peaks can hardly be distinguished experimentally, but the band corresponding to adsorption of two probe molecules at one cation should be noticeably broader than the band for monomolecular adsorption. This is clearly seen in the IR spectra of $^{15}\text{N}_2$ adsorbed on NaY and Na-EMT zeolites [14,16]. The mean blue-shift of the two N–N bands for bimolecular adsorption at the cluster Na–Al-2p, 16.9 cm^{-1} for $^{14}\text{N}_2$ and 16.6 cm^{-1} for $^{15}\text{N}_2$, is by about 4 cm^{-1} smaller than the shift for monomolecular adsorption, while for K–Al-2p cluster the mean shift of bimolecular adsorption is essentially the same as for monomolecular adsorption. This is in line with experimental observations (also shown in Table 2) where the frequency of the N–N band decreases by $2.0\text{--}3.5\text{ cm}^{-1}$ upon adsorption of a second probe molecule to a Na^+ center in zeolites NaY, NaEMT, and NaETS, while the frequency for a bis-dinitrogen complex on potassium containing zeolites is only by 0.5 cm^{-1} lower than for the corresponding monomolecular adsorption [14–17]. However, one should consider this comparison between calculated and experimental frequency shifts as qualitative only because we modeled the location of the cation only at one type of ring, namely at six-rings with two Al centers. Although this type of position for sodium and potassium cations is dominant in Y zeolite and EMT [20,21,23,39], the cations located at other six-rings or in other crystallographic positions can also influence the IR spectra of adsorbed N_2 probe molecules.

The frequencies of the N–Na and N–K stretching modes in the corresponding complexes with one adsorbed probe molecule $^{14}\text{N}_2$ are 129 and 94 cm^{-1} , respectively (by $2\text{--}3\text{ cm}^{-1}$ lower for $^{15}\text{N}_2$, see Table 2). When two N_2 molecules are adsorbed at a cationic center, the band splits into symmetric and antisymmetric contributions; the frequency splitting is 18

and 5 cm^{-1} for Na–Al-2p and K–Al-2p, respectively (Table 2).

With the adsorption of mixed isotope molecules $^{14}\text{N}\text{--}^{15}\text{N}$, one might expect to distinguish between linear and side-on adsorption of dinitrogen molecules at alkali centers [9]. Symmetric side-on adsorption should produce one N–N peak while linear adsorption is expected to furnish two peaks depending on which isotope atom, ^{14}N or ^{15}N , is coordinated to the alkali cation. In order to check this hypothesis [9], we calculated the frequencies in both orientation of a $^{14}\text{N}\text{--}^{15}\text{N}$ molecule on the cluster models Na–Al-2p and K–Al-2p. The difference in the $\nu(\text{N}\text{--}\text{N})$ frequencies between the two orientations of the probe molecule is only $0.2\text{--}0.3\text{ cm}^{-1}$ (Table 2), which can hardly be distinguished experimentally in the IR spectrum.

3.3. Comparison with experimental studies

The linear correlation in Fig. 2a can be used to estimate the relative intensities of the N–N bands of N_2 molecules adsorbed at different alkali cations from the experimental frequency shifts $\Delta\nu(\text{N}\text{--}\text{N})$ on the two cations, e.g. for Na^+ and Cs^+ :

$$\begin{aligned} \frac{I_{\text{Na}}(\text{N}\text{--}\text{N})}{I_{\text{Cs}}(\text{N}\text{--}\text{N})} &= \frac{\Delta\nu_{\text{Na}}(\text{N}\text{--}\text{N})}{\Delta\nu_{\text{Cs}}(\text{N}\text{--}\text{N})} \\ &= \frac{\nu_{\text{Na}}(\text{N}\text{--}\text{N}) - \nu_0(\text{N}\text{--}\text{N})}{\nu_{\text{Cs}}(\text{N}\text{--}\text{N}) - \nu_0(\text{N}\text{--}\text{N})} \end{aligned} \quad (1)$$

Note that this relation holds also for the calculated values of monomolecular adsorption of the probe molecule at the zeolite cluster models: $I_{\text{Na}}/I_{\text{K}} = 1.36$, $\Delta\nu_{\text{Na}}/\Delta\nu_{\text{K}} = 1.35$ (Table 2).

Application of this relation to experimental data is complicated by the fact that there is no consistent reference value $\nu_0(\text{N}\text{--}\text{N})$ for the vibrational frequency of a N_2 molecule which does not interact with cations in zeolite cages. Yamazaki et al. [38] employed the Raman frequency of dinitrogen in the gas phase, 2331 cm^{-1} [40], as reference for the interpretation of the experimental frequency shifts of N_2 on a series of alkali-exchanged ZSM-5 zeolites. When this reference value is used, the experiments on Cs and Rb containing zeolites show negative shift of the N–N stretching mode (by -1 to -4 cm^{-1}),

while the shift is positive for lighter alkali cations [13,16,36,38]. Note that the calculations for bare cations show positive shifts for linearly adsorbed N_2 on all alkali cations (Table 1). For zeolite ZSM-5 with its narrow channels, this change of sign of the frequency shift has been rationalized [38] by an eventual tilting of the probe molecule due to spatial restrictions by the pore walls in case of large cations. However, the same trend was also observed on the zeolites MOR, EMT, and Y with larger cavities (up to 1.3 nm) [13,16,36]. Moreover, no tilting (and correspondingly no negative frequency shift of the principal band) was observed for CO adsorption on the heavier alkali cations, although a CO molecule is by 3 pm longer than N_2 and the distance M–C is also larger than M–N, both at bare and zeolite embedded cations, see Tables 1 and 2 and [11,37,41].

Analyzing this situation, Zecchina and coworkers [9,13,17,36] hypothesized that the problem is due to the use of the gas phase Raman frequency as reference for N_2 in zeolite materials. They favored the vibrational frequencies of N_2 on silica or in a rare gas matrix, $2321\text{--}2324\text{ cm}^{-1}$, since these values accounts also for the influence of the surrounding on N–N frequency. Indeed, the surrounding (either a rare gas matrix, silica or zeolite framework) likely induces a negative frequency shift by about 10 cm^{-1} of adsorbed with respect to gas phase dinitrogen molecules. In this way, the frequency shift caused by the adsorption at the alkali cations is always positive. The fact that the measured N–N frequency shift depends linearly on the strength of the electric field exerted by the cation (as estimated by $R(M-N)^{-2}$) was used as an additional argument supporting this hypothesis [36]. A similar dependence was observed also for the CO frequency shift on these materials. Thus, the derivation of a reasonable reference frequency for N_2 adsorbed on cation exchanged zeolites is important for the interpretation of the interaction and orientation of probe molecules.

To clarify this problem, we compare the reported experimental data for the series of alkali-exchanged zeolites to the calculated frequency shifts for the corresponding alkali cations (Fig. 3). The experimental frequencies in Fig. 3 refer to $^{14}N_2$ adsorbed on a series of alkali-exchanged mordenites [36] and ZSM-5 zeolite [38], as well as to frequencies for $^{14}N_2$ adsorption on EMT recalculated from the frequen-

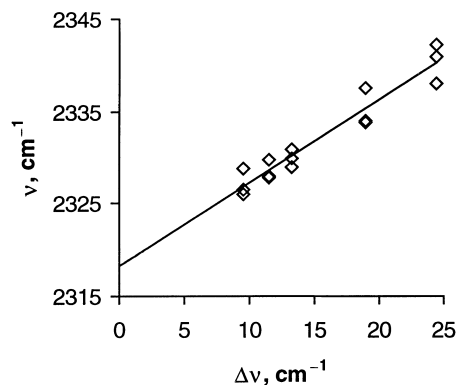


Fig. 3. Experimental frequencies ν of the N–N stretching mode of molecular $^{14}N_2$ adsorbed on a series of alkali-exchanged mordenites [36], ZSM-5 zeolite [38] and EMT (recalculated from the frequencies of $^{15}N_2$) [16] as a function of the calculated frequency shifts $\Delta\nu$ for the bare cation. The straight line intersects the y-axis at 2318 cm^{-1} , the correlation coefficient is 0.93.

cies of $^{15}N_2$ isotope [16]. As can be seen from Fig. 3, the experimental values fit reasonably well to the frequency shifts calculated for bare ions; the correlation coefficient of the straight line including all three data sets is 0.93. If we now extrapolate the (experimental) frequencies to a vanishing calculated shift, we are able to eliminate the shift caused by the coordination of the probe molecule to the alkali cation and, thus, to estimate the frequency shift due to the surrounding zeolite framework. When we combine the data for all three experimental series of alkali cations and extrapolate to $\Delta\nu = 0$, we obtain a value of 2318 cm^{-1} . This frequency can be used as reference $\nu_0(N-N)$ when frequency shifts of $^{14}N_2$ adsorbed on alkali-exchanged zeolites are considered. One can also see that the surrounding zeolite framework induces a frequency red-shift of the N–N mode by about 13 cm^{-1} relative to Raman frequency of N_2 molecule in the gas phase. This line of argument implies that the influence of the zeolite framework on the N_2 vibrational mode is represented by the experimental frequencies used.

An alternative derivation of a reference frequency $\nu_0(N-N)$, that accounts for the influence of the zeolite framework, relies on the linear correlation between the calculated intensities and the frequency shifts of the N–N stretching mode of a dinitrogen molecule coordinated linearly to bare alkali cations (Fig. 2a). If we assume that this correlation holds

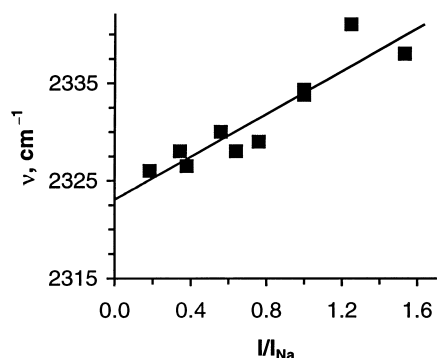


Fig. 4. Correlation between the experimental frequencies ν and the relative intensities I/I_{Na} (with respect to the case of sodium) of the N–N stretching mode of $^{14}\text{N}_2$ adsorbed on a series of alkali-exchanged mordenites [36] and ZSM-5 zeolites [38]. The straight line intersects the y -axis at 2323cm^{-1} , the correlation coefficient is 0.85.

also for the experimental values, the reference frequency ν_0 would correspond to vanishing band intensity. As can be seen from Fig. 4, this assumption seems to hold reasonably well for the reported experimental data for the series of mordenites [36] and ZSM-5 zeolites [38], namely the experimental N–N frequency increases linearly with the relative intensity of the band. From this approach, we find a reference value of 2323cm^{-1} at zero intensity, i.e. the red-shift of the N–N frequency with respect to the gas phase Raman frequency induced by the surrounding is 8cm^{-1} . This value differs by 5cm^{-1} from the reference frequency ν_0 derived by the previous strategy (see Fig. 3). This difference is not unexpected if one takes normal experimental and computational errors into account. The compilation of the experimental data from different sources and framework structures likely also reduces the accuracy of the reference value so derived. For a more precise determination of the reference frequency $\nu_0(\text{N–N})$ based on either approach, it would be highly desirable to have a consistent set of experimental data available, for both isotope molecules $^{14}\text{N}_2$ and $^{15}\text{N}_2$ adsorbed on a series of alkali-exchanged zeolites of the same framework structure, with intensity values measured by one method throughout.

Nevertheless, both approaches for deriving a reference frequency $\nu_0(\text{N–N})$ that accounts for the influence of the zeolite framework show a red-shift of

the N–N mode by about 10cm^{-1} caused by the surrounding, similarly to dinitrogen adsorption on silica. The reference values 2318 and 2323cm^{-1} for $^{14}\text{N}_2$ derived from Figs. 3 and 4 are close to the values proposed by Zecchina and coworkers for $^{14}\text{N}_2$, $2321\text{--}2324\text{cm}^{-1}$ [9,13,36].

If we apply the derived reference values of $\nu_0(\text{N–N})$, 2318 and 2323cm^{-1} , we are able to calculate the experimental frequency shifts for the N–N stretching band in the IR spectra of N_2 adsorbed on specific alkali-exchanged zeolite samples and to estimate the corresponding intensity ratios with the help of Eq. (1). In Table 3, we display the corresponding estimated intensity ratios with respect to I_{Na} based on measured frequency shifts for $^{15}\text{N}_2$ adsorption on EMT zeolites [16] and for $^{14}\text{N}_2$ adsorption on mordenites [36] and ZSM-5 zeolites [38]. For the latter two cases, also the experimental ratios are provided [36,38]. Inspection of Table 3 shows that estimated and experimental intensity ratios exhibit rather similar trends, but the quantitative agreement between the two sets of values is only moderate. Possible reasons are uncertainties in the experimental determination of the extinction coefficient as well as

Table 3

Comparison of calculated and experimental intensity ratios $I_{\text{M}}/I_{\text{Na}}$ of the $\nu(\text{N–N})$ band of dinitrogen adsorbed at alkali cations in various zeolites

Cation	Calculated ^a		$^{15}\text{N}_2$, EMT ^b		$^{14}\text{N}_2$, MOR ^c		$^{14}\text{N}_2$, ZSM5 ^d			
	Calc.	Est. ^e	Est. ^f	Est. ^g	Exp.	Est. ^f	Est. ^g	Exp.	Est. ^f	Est. ^g
Li^+	1.34	1.29	1.24	1.31	1.25	1.44	1.64	1.53	1.25	1.36
Na^+	1.00	1.00	1.00	1.00	1.00	1.00	1.00	1.00	1.00	1.00
K^+	0.73	0.70	0.65	0.55	0.76	0.69	0.55	0.56	0.75	0.64
Rb^+	0.61	0.61	0.59	0.48	0.64	0.63	0.45	0.34	0.63	0.45
Cs^+	0.54	0.50	0.54	0.41	0.38	0.53	0.32	0.19	0.50	0.27

^a Based on the values of bare cations reported in Table 1.

^b Based on experimental data from [16].

^c Based on experimental data from [36].

^d Based on experimental data from [38].

^e Estimated intensity ratio using Eq. (1) and the frequency shifts of adsorbed N_2 with respect to the reference frequency $\nu_0 = 2320.7\text{cm}^{-1}$ calculated for free N_2 molecule.

^f Estimated intensity ratio using Eq. (1) with reference frequency ν_0 ; 2318cm^{-1} for $^{14}\text{N}_2$ and 2240cm^{-1} for $^{15}\text{N}_2$ estimated from Fig. 3.

^g Estimated intensity ratio using Eq. (1) with reference frequency ν_0 ; 2323cm^{-1} for $^{14}\text{N}_2$ and 2244cm^{-1} for $^{15}\text{N}_2$ estimated from Fig. 4.

limitations of the cluster model calculations and the computational method used.

4. Conclusions

In the present computational study, we estimated binding energies and adsorption induced frequency shift of N_2 probe molecules adsorbed on alkali-exchanged zeolites. In all cases, both on bare cations and at zeolite model clusters, a linear configuration M–N–N for the adsorption complexes of the probe molecule at the metal cation was found as the most stable one. In these complexes, the stretching mode $\nu(N-N)$ is blue-shifted by 10–25 cm^{-1} compared to the value calculated for a N_2 molecule in the gas phase. The frequency shifts $\Delta\nu(N-N)$ and intensities $I(N-N)$ of the stretching mode were found to correlate in linear fashion for the series of alkali cations. Application of this correlation to reported experimental data allowed us to extract a reference vibrational frequency $\nu_0(N-N)$ for a N_2 molecule in zeolite cages non-interacting with cations, 2323 cm^{-1} . Another possibility to estimate such a reference value is based on the observed proportionality between experimental frequencies of N_2 adsorbed on three series of alkali-exchanged zeolites and the calculated frequency shifts for the corresponding cations. The reference value for non-interacting N_2 molecule derived from this correlation is 2318 cm^{-1} for $^{14}N_2$. Both approaches showed that the surrounding zeolite framework induces red-shift of the N–N frequency with respect to the gas phase Raman frequency by about 10 cm^{-1} . A more precise determination of the reference frequency requires a consistent set of experimental data for both isotope molecules $^{14}N_2$ and $^{15}N_2$ adsorbed on the same series of alkali-exchanged zeolites, with intensity values measured by a uniform method.

Our computational results support the experimental observation of Hadjiivanov and Knözinger [14–16] concerning the simultaneous adsorption of two N_2 molecules at one alkali cation. The adsorption energy of the second molecule is by only 1–2 kJ/mol lower than the binding energy of the first probe molecule. The calculated frequency shifts of the stretching vibrational mode of the bis-dinitrogen

complex at a Na-exchanged zeolite is by 4 cm^{-1} lower than for the corresponding monomolecular adsorption complex while the position of the bands is almost unchanged for K-exchanged zeolite, in good agreement with the experimental findings.

Acknowledgements

We would like to thank Prof. H. Knözinger for a long-standing productive collaboration on many topics of mutual interest and for generously sharing his insights on catalysis. We are indebted to him for bringing the problems connected with the characterization of alkali-exchanged zeolites to our attention. We also thank Dr. K. Hadjiivanov for fruitful discussions and Dr. K. Neyman for helpful comments. G.N.V. gratefully acknowledges a fellowship of the Alexander von Humboldt Foundation. This work was supported by the Deutsche Forschungsgemeinschaft and the Fonds der Chemischen Industrie.

References

- [1] D. Barthomeuf, *Catal. Rev.* 38 (1996) 521.
- [2] C. Bezoukhanova, Yu. Kalvachev, *Catal. Rev.* 36 (1994) 125.
- [3] H. Förster, H. Fuess, E. Geidel, B. Hunger, H. Jobic, C. Kirschhock, O. Klepel, K. Krause, *Phys. Chem. Chem. Phys.* 1 (1999) 593.
- [4] G.N. Vayssilov, J.A. Lercher, N. Rösch, *J. Phys. Chem. B* (2000) in press.
- [5] H. Knözinger, Y. Zhao, B. Tesche, R. Barth, R. Epstein, B.C. Gates, J. Scott, *Faraday Discuss.* 72 (1981) 53.
- [6] H.-P. Böhm, H. Knözinger, in: J.R. Anderson, M. Boudart (Eds.), *Catalysis — Science and Technology*, Vol. 4, Springer, Berlin, 1983, p. 39.
- [7] H. Knözinger, in: G. Ertl, H. Knözinger, J. Weitkamp (Eds.), *Handbook of Heterogeneous Catalysis*, Vol. 2, Wiley-VCH, Weinheim, 1997, p. 707.
- [8] H. Knözinger, S. Huber, *J. Chem. Soc., Faraday Trans.* 94 (1998) 2047.
- [9] A. Zecchina, C. Otero Arean, *Chem. Soc. Rev.* 25 (1996) 187.
- [10] G.N. Vayssilov, N. Rösch, *J. Catal.* 186 (1999) 423.
- [11] G.N. Vayssilov, M. Staufer, T. Belling, K.M. Neyman, H. Knözinger, N. Rösch, *J. Phys. Chem. B* 103 (1999) 7920.
- [12] E. Cohen de Lara, Y. Delaval, *J. Chem. Soc., Faraday Trans.* 2 (74) (1978) 790.
- [13] G.L. Marta, A.N. Fitch, A. Zecchina, G. Riccardi, M.

- Salvalaggio, S. Bordiga, C. Lamberti, *J. Phys. Chem. B* 101 (1997) 10653.
- [14] K. Hadjiivanov, H. Knözinger, *Chem. Phys. Lett.* 303 (1999) 513.
- [15] K. Hadjiivanov, H. Knözinger, *Catal. Lett.* 58 (1999) 21.
- [16] K. Hadjiivanov, P. Massiani, H. Knözinger, *Phys. Chem. Chem. Phys.* 1 (1999) 3831.
- [17] A. Zecchina, C. Otero Arean, G. Turnes Palomino, F. Geobaldo, C. Lamberti, G. Spoto, S. Bordiga, *Phys. Chem. Chem. Phys.* 1 (1999) 1649.
- [18] K.M. Neyman, P. Strodel, S.Ph. Ruzankin, N. Schlensog, H. Knözinger, N. Rösch, *Catal. Lett.* 31 (1995) 273.
- [19] P.J. O'Malley, K.J. Farnworth, *J. Phys. Chem. B* 102 (1998) 4507.
- [20] J. Klinowski, S. Ramdas, J.M. Thomas, *J. Chem. Soc., Faraday Trans. 2* (78) (1982) 1025.
- [21] M.T. Melchior, D.E.W. Vaughan, A.J. Jacobson, *J. Am. Chem. Soc.* 104 (1982) 4859.
- [22] S. Huber, H. Knözinger, *Appl. Catal. A* 181 (1999) 239.
- [23] A.N. Fitch, H. Jobic, A. Renouprez, *J. Phys. Chem.* 90 (1986) 1311.
- [24] T. Belling, T. Grauschopf, S. Krüger, F. Nörtemann, M. Staufer, M. Mayer, V.A. Nasluzov, U. Birkenheuer, A. Hu, A.V. Matveev, N. Rösch, PARAGAUS 2.1, Technische Universität München, München, 1999.
- [25] A.D. Becke, *Phys. Rev. A* 38 (1988) 3098.
- [26] J.P. Perdew, *Phys. Rev. B* 33 (1986) 8822; 34 (1986) 7406.
- [27] A. Schäfer, C. Huber, R. Ahlrichs, *J. Chem. Phys.* 100 (1994) 5829.
- [28] A.M. Ferrari, K.M. Neyman, N. Rösch, *J. Phys. Chem. B* 101 (1997) 9292.
- [29] P.J. Hay, W.R. Wadt, *J. Chem. Phys.* 82 (1985) 299.
- [30] A. Hu, M. Staufer, U. Birkenheuer, V. Igoshine, N. Rösch, *Int. J. Quantum Chem.* 79 (2000) 209.
- [31] V.A. Nasluzov, N. Rösch, *Chem. Phys.* 210 (1996) 413.
- [32] A. Görling, S.B. Trickey, P. Gisdakis, N. Rösch, in: J. Brown, P. Hofmann (Eds.), *Topics in Organometallic Chemistry*, Vol. 4, Springer, Heidelberg, 1999, p. 109.
- [33] R.A. van Santen, *Catal. Today* 38 (1997) 377.
- [34] P.S. Bagus, G. Pacchioni, C. Nelin, in: R. Carbo (Ed.), *Quantum Chemistry: Basic Aspects, Actual Trends*, Elsevier, Amsterdam, 1989, p. 475.
- [35] G. Pacchioni, G. Cogliandro, P.S. Bagus, *Int. J. Quantum Chem.* 96 (1992) 1115.
- [36] F. Geobaldo, C. Lamberti, G. Ricchardi, S. Bordiga, A. Zecchina, G. Turnes Palomino, C. Otero Arean, *J. Phys. Chem.* 99 (1995) 11167.
- [37] A.M. Ferrari, K.M. Neyman, N. Rösch, *J. Phys. Chem. B* 101 (1997) 9292.
- [38] T. Yamazaki, I. Watanuki, S. Ozawa, Y. Ogino, *Bull. Chem. Soc. Jpn.* 61 (1988) 1039.
- [39] J.L. Lievens, J.P. Verduijn, A.J. Bons, W.J. Mortier, *Zeolites* 12 (1992) 698.
- [40] F. Rasetti, *Phys. Rev.* 34 (1929) 367.
- [41] A.M. Ferrari, P. Ugliengo, E. Garone, *J. Chem. Phys.* 105 (1996) 4129.